Combined stent-retriever and aspiration intra-arterial thrombectomy performance for fragmentable blood clots

A proof-of-concept computational study

Luraghi, Giulia; Bridio, Sara; Lissoni, Vittorio; Dubini, Gabriele; Dwivedi, Anushree; McCarthy, Ray; Fereidoonnezhad, Behrooz; McGarry, Patrick; Gijsen, Frank J.H.; More Authors

DOI
10.1016/j.jmbbm.2022.105462

Publication date
2022

Document Version
Final published version

Published in
Journal of the mechanical behavior of biomedical materials

journal of the mechanical behavior of biomedical materials 135 (2022) 105462

Contents lists available at ScienceDirect

Journal of the Mechanical Behavior of Biomedical Materials

journal homepage: www.elsevier.com/locate/jmbbm

Combined stent-retriever and aspiration intra-arterial thrombectomy performance for fragmentable blood clots: A proof-of-concept computational study

Giulia Luraghi [a,b,*], Sara Bridio [a], Vittorio Lissoni [a], Gabriele Dubini [a], Anushree Dwivedi [c], Ray McCarthy [c], Behrooz Fereidoonnezhad [b,d], Patrick McGarry [d], Frank J.H. Gijsen [b,e], Jose Felix Rodriguez Matas [a], Francesco Migliavacca [a]

[a] Department of Chemistry, Materials and Chemical Engineering "Giulio Natta", Politecnico di Milano, Milan, Italy
[b] Department of Biomechanical Engineering, Delft University of Technology, Delft, the Netherlands
[c] Cerenovus, Neuro Technology Center, Galway, Ireland
[d] Department of Biomedical Engineering, National University of Ireland Galway, Galway, Ireland
[e] Department of Biomedical Engineering, Thoraxcenter, Erasmus Medical Center, Rotterdam, the Netherlands

ARTICLE INFO

Keywords:
Thrombectomy
Acute ischemic stroke
Stent-retriever
Finite element analysis

ABSTRACT

Mechanical thrombectomy (MT) treatment of acute ischemic stroke (AIS) patients typically involves use of stent retrievers or aspiration catheters alone or in combination. For in silico trials of AIS patients, it is crucial to incorporate the possibility of thrombus fragmentation during the intervention. This study focuses on two aspects of the thrombectomy simulation: i) Thrombus fragmentation on the basis of a failure model calibrated with experimental tests on clot analogs; ii) the combined stent-retriever and aspiration catheter MT procedure is modeled by adding both the proximal balloon guide catheter and the distal access catheter.

The adopted failure criterion is based on maximum principal stress threshold value. If elements of the thrombus exceed this criterion during the retrieval simulation, then they are deleted from the calculation.

Comparison with in-vitro tests indicates that the simulation correctly reproduces the procedures predicting thrombus fragmentation in the case of red blood cells rich thrombi, whereas non-fragmentation is predicted for fibrin-rich thrombi. Modeling of balloon guide catheter prevents clot fragments' embolization to further distal territories during MT procedure.

1. Introduction

In five recent randomized clinical trials (Berkhemer et al., 2015; Chalumeau et al., 2018; Goyal et al., 2015; Jovin et al., 2015; Saver et al., 2015) the intra-arterial mechanical thrombectomy (MT) proved to be a safe and effective treatment for acute ischemic stroke (AIS); MT is now considered the standard of care for AIS patients with large vessel occlusion. MT consists of the mechanical removal of a thrombus (blood clot) from a cerebral artery. MT techniques can be performed with stent-retrievers, large bore aspiration catheters, or a combination of both devices(Kühn et al., 2020). The combined approach with stent-retriever and aspiration is recently associated with a trend of higher successful vessel recanalization (Kang et al., 2013). However, the risk of thrombus fragmentation is still present and needs to be curtailed to avoid emboli and micro-emboli obstructing the downstream cerebral vessels.

During the MT with stent-retriever, the thrombus is engaged by deploying the device at the thrombus location, once the thrombus is removed the blood flow is restored in the vessels Different techniques can be used when deploying and removing the stent-retriever in combination with different catheters (Munich et al., 2019). Examples of widespread clinical techniques are the Solumbra (Combined Stent Retriever and Suction Thrombectomy) (Deshaies, 2013; Dumont et al., 2014; Humphries et al., 2015), the ARTS (Aspiration-retriever technique for stroke) (Massari et al., 2016), the CAPTIVE (continuous aspiration prior to intracranial vascular embolectomy) (McTaggart et al., 2017), the SAVE (Stent retriever assisted vacuum-locked extraction) (Maus et al., 2018) and the BADDASS (Balloon guide with large-bore distal

* Corresponding author.
E-mail address: giulia.luraghi@polimi.it (G. Luraghi).

https://doi.org/10.1016/j.jmbbm.2022.105462
Received 27 June 2022; Received in revised form 29 August 2022; Accepted 8 September 2022
Available online 14 September 2022

access catheter with dual aspiration with stent-retriever as standard approach) (Ospel et al., 2019) approaches.

Some of the ancillary devices involved in the MT procedure include the microcatheter (around 0.5 mm in diameter), the stent-retriever (between 4 and 6 mm in diameter), the (balloon) guide catheter (around 2.6 mm in diameter), and the distal access catheter (around 1.6 mm in diameter). In the clinical procedure, once the guidewire creates the path, the microcatheter is advanced to the thrombus location in order to place the crimped stent-retriever. Stent-retriever is a self-expandable stent made of nickel-titanium alloys, a superelastic material which, once crimped with high deformations, can return to its original shape simply by removing the microcatheter. Once the stent-retriever is deployed across the thrombus, the distal access catheter (DAC) is advanced to face the thrombus. The stent is then completely retracted into the DAC under continuous aspiration or only partially retracted into the DAC under continuous aspiration. In the latter, the DAC and the stent-retriever are retracted as a unit. The guide catheter is normally placed in the cervical internal carotid artery (ICA) and receives the stent-retriever and/or the DAC with the removed thrombus. It can be used to apply proximal aspiration. The guide catheter can incorporate a balloon to be inflated during the procedure and in this case, it is referred to as the balloon guide catheter (BGC). The clinical use of the BGC which causes a momentary blockage of the antegrade blood flow during the procedure is now preferred over conventional guide catheters to prevent embolic events and to speed up the MT procedure (Chueh et al., 2020).

There is an increasing interest in virtually reproducing clinical procedures. For device manufacturing companies to speed-up development and optimize new devices; for clinicians to improve pre-operative planning and as a predictive clinical tool; finally, to replace animal experimentation, and to improve the outcomes of clinical trials. In this view, it is important to assess the credibility of computational models of clinical procedures. Once the models are used in a specific context of use, validation evidence is required to build and prove the credibility of simulations (Luraghi et al., 2021a). The context of use here is to simulate the MT procedure with combined stent-retriever and aspiration catheters (BGC and/or DAC) in virtual patients in order to predict the procedure outcome.

Regarding the MT procedure, few studies model the mechanical behavior of single devices, stent-retrievers (Gu et al., 2017; Liu et al., 2021; Mousavi et al., 2021) or aspiration catheters (Chitsaz et al., 2018; Fereidoonnezhad and McGarry, 2021; Good et al., 2020; Oyekole et al., 2021; Shi et al., 2017), in idealized straight or curved vessels, an over-simplified geometry in comparison with the geometry of the ICA, which is characterized by a complex morphology (Bridio et al., 2021). Recently, our group developed and validated the first virtual MT with stent-retriever in real vessel morphologies using in vitro tests (Luraghi et al., 2021d) and clinical data(Luraghi et al., 2021b).

In this work, a combined in silico MT with stent-retriever and aspiration catheters, using both BGC and DAC, is developed and qualitatively validated with in-vitro experiments, as a first step toward building a credibility analysis of the virtual procedure. With respect to the previously developed in silico methodology replicating the MT procedure with stent-retriever only (Bridio et al., 2021; Luraghi et al., 2021b, 2021d), two new aspects have been further developed and added in this study. Firstly, the thrombus has non-symmetric tensile and compression behavior, and it can fragment successfully due to the addition of a failure model calibrated with experimental data. Secondly, the combined stent-retriever and aspiration catheter MT procedure is modeled by adding both the proximal BGC and the DAC aspirations to the MT with stent-retriever.

2. Materials and methods

2.1. Thrombus modeling

Clot analogs were obtained from venous whole ovine blood (Duffy et al., 2017; Weafer et al., 2019). Fereidoonnezhad et al. (Fereidoonnezhad et al., 2021a, 2021b) performed unconfined compression tests (Fig. 1a) and tension tests on blood clots made from 5%, 20%, and 40% Hematocrit (%H) blood mixture. They used the inverse finite element method to identify the material properties of the blood clot from these tests. In the current study, we reproduce the uniaxial tension/-compression curves from the material parameters reported in Fereidoonnezhad et al. (2021a). The experimental tests were numerically reproduced using a simplified phenomenological quasi-hyperelastic foam model (Kolling et al., 2007) implemented in the software LS-DYNA R13 (ANSYS, Canonsburg, PA, USA). As in the classical Hill-Odgen formulation, the principal components of the Kirchhoff stress are a function of the principal stretches. However, in this case, the function is directly determined from the uniaxial experimental curves without an analytical expression. The Poisson's ratio was set to 0.3 after a calibration procedure (Luraghi et al., 2021d). The performance of this model to replicate both the compression and tensile experimental curves is shown in Fig. 1c.

A failure model for clots, which reproduces the fracture tests (Fig. 1b) is also incorporated to predict clot fragmentation during mechanical thrombectomy. The failure criterion is based on the maximum principal stress (PSMAX). The elements exceeding the PSMAX threshold during the simulation are deleted from the calculation, allowing to generate fragments and discontinuities in the clot. The maximum PSMAX at failure for each clot content was identified by calibrating the model with experimental data of the tension fracture tests(Fereidoonnezhad et al., 2021a). The performance of this failure model to replicate the fracture experimental curves is shown in Fig. 1d. The PSMAX at failure values was set as 0.037 MPa, 0.073 MPa, and 0.1 MPa for clots with 5%H, 20%H, and 40%H, respectively.

2.2. In vitro MT tests with combined techniques

Three different MT procedures were performed in the same vessel-like 3D-printed silicone phantom. The 3D phantom was designed in order to replicate the physiological dimension of the cerebral arteries. For these experiments, two clot compositions were used that represent low and high fibrin content in the clot by histology. Red blood cell (RBC)-rich clots were prepared with estimated 40%H content and fibrin-rich clots with 5%H content approximately. The RBC-rich clot measured 12 mm in length and 4 mm in diameter when lodged in the silicone model for the first MT experiment (MT1), whereas fibrin-rich (FIB) clots measured 7.5 mm in length and 4 mm in diameter for the other two thrombectomy experiments (MT2 and MT3). All the clots were lodged in the same location of the middle cerebral artery. Saline was circulated through the model at 37 °C and flow arrest was achieved by blocking the flow in the ICA. In particular, (i) MT1 was designed with only BCG aspiration catheters and RBC-rich clot, (ii) MT2 with again only BCG but FIB-rich clot, and (iii) MT3 with both DAC and BCG aspiration catheters and FIB-rich clot.

In all the performed procedures, the Rebar 18 (Medtronic, Ireland) micro-catheter was used to place and deploy the EmboTrap II (ET II, Cerenovus, Ireland) stent-retriever at the thrombus location. Proximal aspiration through the BGC Neuron Max 088 (Penumbra, CA, USA) was applied using a 60 ml syringe, once for each pass during the procedures. Only for MT3, distal aspiration was also applied through the Sofia Plus (MicroVention, Inc., CA, USA) DAC using a 60 ml syringe once during the procedure. All retrievals were recorded with a CCD camera. The experiments performed are summarized in Table 1.

2.3. In silico MT tests with combined techniques

The CAD model of the 3D-printed patient-like cerebral vasculature was processed and discretized with quadrilateral rigid elements (Luraghi et al., 2021d). The two clot analogs used in the experiments were virtually reproduced. The geometries were discretized with linear

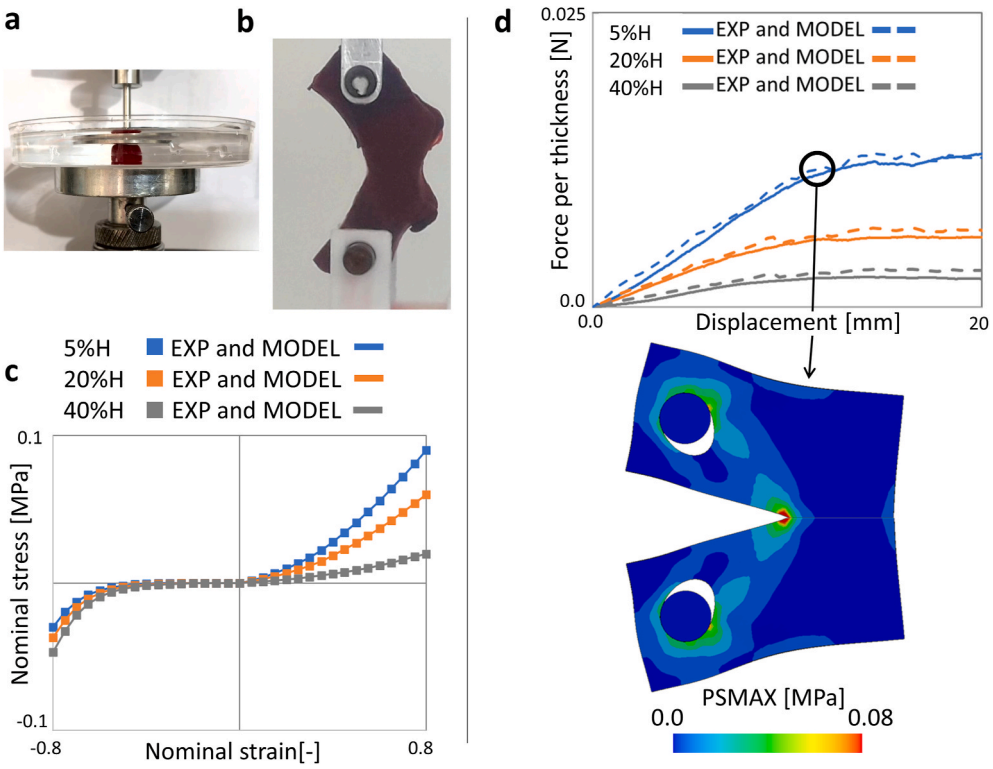

Fig. 1. Tensile and compression in vitro (a) and in silico tests of clots to validate the adopted foam material model (c); fracture in vitro (b) and in silico tests to define the maximum principal stress values (PSMAX) at failure for different clot compositions (d).

Table 1
Description of the three in vitro combined stent-retriever and aspiration MT performed procedures. RBC: red blood cell, FIB: fibrin; ET II: EmbrTrap II (5 × 37 mm); BGC: balloon guide catheter; DAC: distal access catheter; MT: mechanical thrombectomy.

Test	CLOT			MT procedure		
	Clot type	Clot length	Clot size	Stent	BGC	DAC
MT1	RBC Rich	12 mm	4 mm	ET II	Neuron Max 088	–
MT2	FIB Rich	7.5 mm	3.5 mm	ET II	Neuron Max 088	–
MT3	FIB Rich	7.5 mm	3.5 mm	ET II	Neuron Max 088	Sofia Plus

tetrahedral elements and the material was modeled as a compressible foam with failure as described in the previous paragraph. A mass proportional damping of 10 s^{-1} was applied to the thrombus model (Luraghi et al., 2021d) in order to smooth the frequency vibration without introducing numerical artificial viscosity. The EmboTrap II stent-retriever model was created by pre-processing the CAD geometry and by discretizing it with Hughes-Liu beam elements (Fig. 2a) (Luraghi et al., 2022). The Ni–Ti stent material was modeled with a shape memory alloy behavior and the material parameters were obtained by calibrating to the experimental data of the uniaxial tensile test, as described in our previous work (Luraghi et al., 2021d) (the material parameters are listed in Appendix 2). Self-penalty contact was used to prevent inter-penetration. A mass proportional damping of 1 s^{-1} was applied to the stent model.

Both the micro-catheter and the BGC were modeled as cylinders of diameter 0.5 mm and 2.3 mm respectively and were discretized with quadrilateral rigid. On the contrary, the DAC with a diameter of 1.8 mm was discretized with quadrilateral deformable shell elements since it is retrieved with the stent. An orthotropic linear elastic model was adopted for the DAC in order to have a higher circumferential stiffness with respect to the longitudinal one(Wang et al., 2019), mimicking the braided metallic-reinforce real DAC device (the material parameters are listed in Appendix 2). A mass proportional damping of 1 s^{-1} was applied to the DAC model.

All the discretized models (vessel, thrombus, stent, and catheters) have an averaged-element size of 0.2 mm in order to facilitate stability of the contact interactions after a sensitivity mesh size analysis(Luraghi et al., 2021d). The total number of elements and nodes for each model is reported in Table 2.

Three MT in silico tests (MT1, MT2, and MT3) were implemented by reproducing the three MT in vitro tests according to the different combined procedures used. Thrombi were positioned at the same middle cerebral artery location as the experiments. A selective mass scaling was adopted in order to fix the time-step of $7{\cdot}10^{-7}$ s. Satisfaction of the quasi-static condition was verified in all the simulations to guarantee the soundness of the time step.

The MT with combined stent-retriever and aspiration consisted of the following steps:

I. Stent crimping & micro-catheter tracking. The stent-retriever was crimped to 0.5 mm in a straight and rigid catheter. A penalty frictionless contact was defined between the stent and the catheter. At the same time, the thrombus was deformed against the vessel wall by tracking the micro-catheter whose position was designed to be similar to the experimental one (Fig. 2b). A penalty contact with 0.4 of friction (Gunning et al., 2018) was defined between the thrombus surface and the vessel wall (after a sensitivity analysis performed in (Luraghi et al., 2021d))
II. Stent tracking. The crimped stent-retriever was pulled within the micro-catheter until reaching the thrombus location. The relative position of the stent with respect to the thrombus was set to match that of the experiments (Fig. 2c).

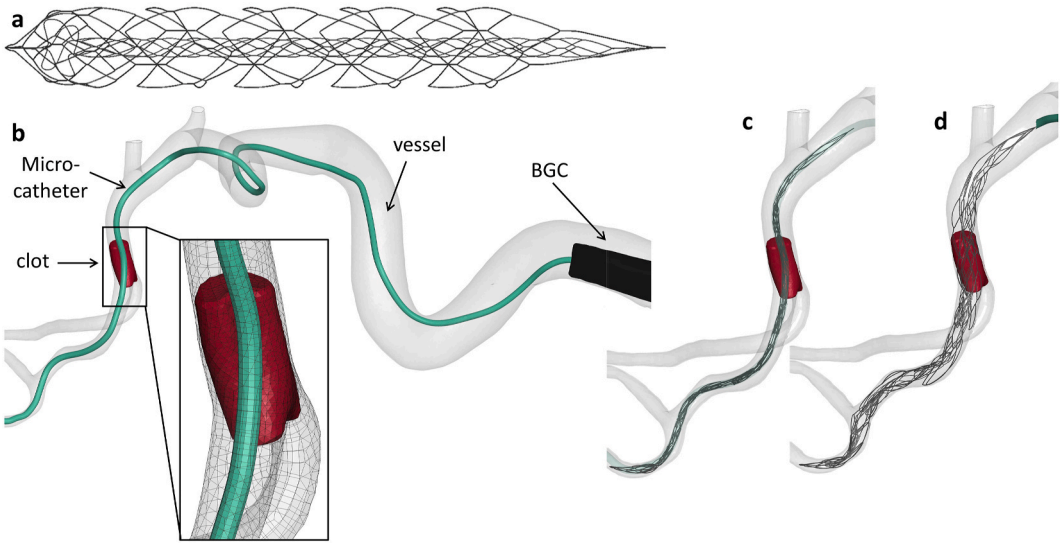

Fig. 2. ET II finite-element stent-retriever model (a); during the first step of the simulation the micro-catheter (in light-green) is placed and squeezed the clot (in red) against the vessel wall (b). To follow, the crimped stent-retriever tracking (c) and its deployment (d).

Table 2
Total number of elements and nodes for each component.

Model	Average size	Total number of elements	Total numer of nodes
Stent-retriever	0.2 mm	4,351	4,228
Thombus	0.2 mm	MT1: 34,483 MT2 and MT3: 18,945	MT1: 7,016 MT2 and MT3: 3,922
Vessel	0.2 mm	21,143	21,085
micro-catheter	0.2 mm	10,092	10,089
BCG	0.2 mm	6,615	6,656
DAC	0.2 mm	17,115	17,075

III. Stent deployment (and DAC tracking if needed). The crimped and placed stent-retriever was deployed by progressively removing the contact with the micro-catheter to mimic the real unsheathing procedure (Fig. 2d). Penalty contacts were activated between the stent and the thrombus and between the stent and the vessel wall with a friction of 0.2 and no friction, respectively. In the MT3 test, once the stent was completely deployed, the DAC was advanced and placed in contact with the proximal face of the thrombus. Penalty contacts were activated between the DAC and the thrombus (friction of 0.2), between the DAC and the stent (frictionless), and between the DAC and the vessel wall (frictionless).

IV. Retrieval. The stent-retriever with the entrapped thrombus (and eventually the DAC in MT3) were retrieved together. During the retrieval phase of the MT3 test, a constant negative pressure of 80 kPa (Froehler, 2017) was applied to the thrombus portion inside the DAC mimicking the syringe aspiration(Nikoubashman et al., 2018). In all models, the thrombus surface exposed toward the BGC and not occupied by the DAC was subjected to the BGC aspiration pressure. This pressure was not constant along with the simulation, with its magnitude being a linear function of the distance between the thrombus and the BGC. This function was estimated by means of a sensitivity computational fluid-dynamics analysis as detailed in Appendix 1. Penalty contacts were activated between the BGC and the thrombus and between the BGC and the stent wall with the friction of 0.2 and no friction, respectively.

All models were built in ANSA PreProcessor v22.0 (BETA CAE System, Switzerland) and solved with the finite-element solver LS-DYNA R13 (ANSYS, Canonsburg, PA, USA). Simulations were carried out on 28 CPUs of an Intel Xeon64 with 250 GB of RAM and lasted from 19 to 27 h.

3. Results

Simulations of the tensile, compression and fracture tests on clot analogs were carried out to verify and validate the clot/thrombus material model (Fig. 1). These in vitro/in silico tests on clot mechanical performance can be used to extract/interpolate the behavior also for clots with different %H content.

The three presented in vitro MT tests are selected in order to show different aspects and were numerically produced. Qualitative comparison in terms of the structure deformation (stent and thrombus position and motion) was performed. Evaluation of the evolution of the maximum principal stress in the thrombus during the MT simulations was analyzed and discussed.

In MT1 the RBC-rich thrombus fragmented during the retrieval phase of the procedure but remained trapped within the outer cage of the stent-retriever and was completely aspirated through the BGC (Fig. 3).

The model replicated the fragmentation of the thrombus during the retrieval as the maximum PSMAX in the clot exceed the maximum PSMAX at failure (0.037 MPa) as shown in Fig. 4. The aspiration pressure applied through the BGC enabled the fragments to be removed without any bulky embolization. For the sake of this example, the same simulation but without the failure model was carried out. As expected, the thrombus behaved in the same way as the original simulation up to the breaking point (because the response is elastic and no elements have been removed yet), then it was completely and entirely removed. Differences are visible between the PSMAX curves from simulations with and without the failure mode (Fig. 4). It must be noted that in the original MT1 simulation the elements with stress higher than 0.037 MPa are deactivated and not considered in the curve of Fig. 4.

MT2 and MT3 were selected and compared because they present the same MT settings (in terms of thrombus position, length, and composition) but with a single aspiration via the BGC (test MT2) and a double aspiration via both the BGC and DAC (test MT3). Both the experiments were truthfully replicated by the in silico model. In MT2 (Fig. 5) the thrombus slides towards the tail of the stent-retriever during the retrieval phase but it was successfully aspirated by the BGC. In MT3 (Fig. 6) the thrombus remained attached to the DAC during the retrieval until reaching the BGC. Differences between the PSMAX curves from

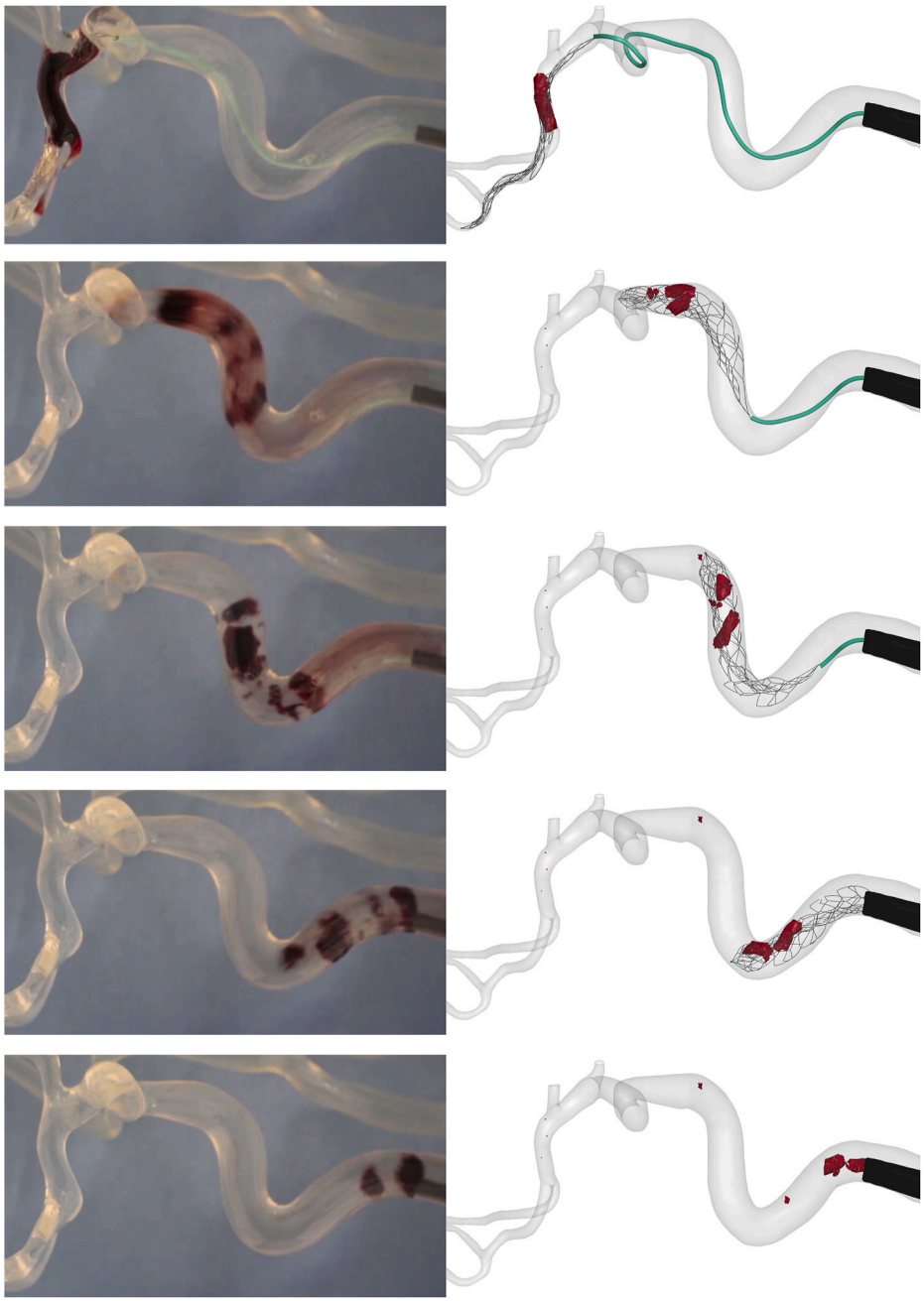

Fig. 3. Comparison between the in vitro (left panel) and the in silico (right panel) MT1 test. The simulation is able to replicate the clot fragmentation.

MT2 and MT3 are visible in Fig. 7. The curve from MT2 is more uniform showing two increments in the PSMAX, the first during stent deployment at the beginning of the retrieval and the second during the final aspiration in the BGC. Differently, the curve from MT3 presents different peaks during the retrieval because of the presence of the DAC.

4. Discussion

In silico models are very widespread today to reproduce, study, evaluate and improve clinical procedures. Since the question of interest is to reproduce a procedure on virtual patients, in silico models need to be truthful in reproducing the reality and a credibility assessment is required. Factors to build model credibility involve validation evidence. This work aimed at developing in silico MT procedures which combined stent-retriever and aspiration catheters.

The aspiration is introduced in the MT to reduce the risk of embolization in case of thrombus fragmentation during the procedure. The risk of thrombus fragmentation is related to its composition (Kaesmacher et al., 2017) and thrombus mechanical properties are strongly correlated with the composition (Gersh et al., 2009). For this reason, a compressible hyperelastic formulation was here adopted to model the non-symmetric behavior in tension and compression observed from the experimental mechanical characterization of different clot analogs. In the literature, some thrombus models have been proposed employing both fluid (Neidlin et al., 2016) and solid (Chitsaz et al., 2018; Talayero et al., 2020) approaches, compressible, hyperelastic, viscoelastic, and fibrin network properties. However, these models were not used to virtual reproduce the complete MT procedure, because of its complexity from a numerical point of view. Recently, a particle approach has been used to model the thrombus subjected to high deformations during an MT but without considering a failure mode and without any material validation against experimental data (Mousavi J S et al., 2021). In this

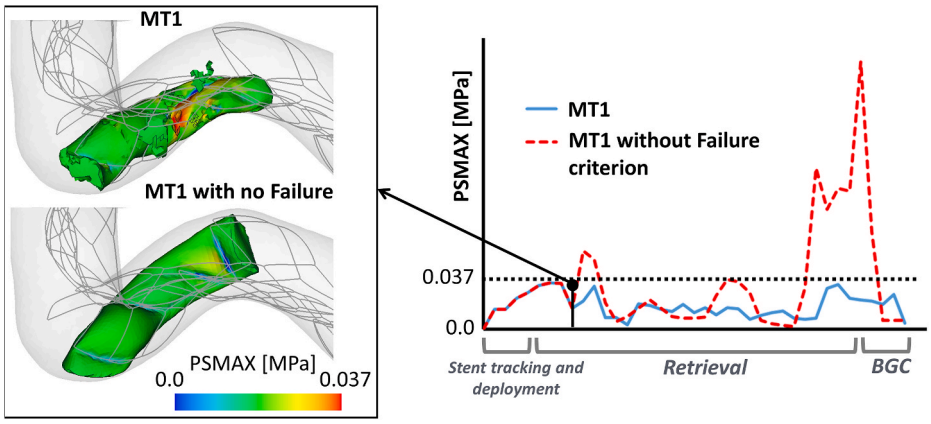

Fig. 4. Right: maximum PSMAX over time during the MT1 simulation with and without the failure model. Left: PSMAX contour plots on the thrombus at the time when the failure starts in MT1. Dotted line: PSMAX failure values for RBC-rich thrombi. In the original MT1 simulation, the elements with stress higher than 0.037 MPa are deactivated and not considered in the relative curve.

work instead, a failure model based on the maximum principal stress calibrated with experimental data was implemented to replicate the possibility of thrombus fragmenting during the virtual MT procedure.

The limited number of in silico studies on the MT is because the accurate implementation of the procedure poses a particular challenge due to the interaction between different deformable parts with different material properties (Luraghi et al., 2021c) among them. The contact between the metallic frame of the stent-retriever and the compliant and bulky thrombus is computationally expensive, in particular, if the stent is moving in a tortuous vessel as in the retrieval phase of the MT procedure. For this reason, MT models in a patient-like vessel are rare in the literature (Bridio et al., 2021; Luraghi et al., 2021b, 2021d). On the other side, aspiration catheters for MT have been always modeled as rigid component (Chitsaz et al., 2018; Fereidoonnezhad and McGarry, 2021; Good et al., 2020; Neidlin et al., 2016; Oyekole et al., 2021; Shi et al., 2017), and their performance has been usually evaluated by means of computational fluid dynamics simulations. Differently, the interaction between the aspiration catheter and the thrombus is modeled in structural simulations with different approaches (Chitsaz et al., 2018; Fereidoonnezhad and McGarry, 2021; Good et al., 2020; Oyekole et al., 2021) through simplified and idealized models. In this work, for the first time, an aspiration catheter is modeled as a deformable structure interacting with the clot during the virtual MT procedure with stent-retrievers.

Thrombus fragments are expected consequences of MT, in particular during the retrieval phase when the stent-retriever and the embedded thrombus are retracted into a receiver catheter (Chueh et al., 2020) (conventional guide catheter, BGC, or DAC depending on the procedures).

In this study, three MT experiments were conducted and virtually reproduced. In-silico MT procedure with a blood cells rich thrombus demonstrated the ability of the proposed thrombus model to fragment during the retrieval phase, reproducing the experiment. Moreover, it was shown how the modeling of BGC prevents the fragments' embolization to further distal position within the vessel tree.

On the contrary, the in-silico MT procedure with fibrin-rich thrombus did not produce fragmentation also when a DAC is used (MT3 model). The different MT techniques were compared in terms of thrombus kinematics and stresses. As expected, the use of the DAC in MT3 increases the stress on the thrombus during the retrieval and may induce fragmentation of the thrombus in the case of RBC-rich clots.

As in all validation studies, some differences between the context of use of the model (reproduce virtual MTs in virtual patients) and the validation evidence are present as already thoroughly described, i.e. the vessel, thrombus geometry, and material(Luraghi et al., 2021a).

Regarding the limitations of this study, it is noteworthy to underline that the comparison between in vitro and in silico MTs is mainly qualitative. However, since the model aims at predicting the procedural outcome in terms of thrombus removal (and blood flow restored) without any variable quantification, we believe that the proposed comparison is adequate as a first step toward the validation of the virtual MT outcome but there is still room for doing additional experiments for a stronger validation evidence. Secondly, the negative pressure generated by the syringes (manually used), was calibrated with a sensitivity CFD analysis based on literature parameters instead of values measured during the experiments. Hence, aspiration boundary conditions may differ from the in vitro and in silico procedures indeed. Thirdly, some assumptions for the thrombectomy simulations have been adopted because data are still missing in the current state-of-the-art as the mechanical performance and characterization of the DACs, friction behavior between stent and vessel, between the catheters and the vessel, and between the catheters and the clots. All these points are potential differences between in vitro and in silico procedures. In the future, more efforts should be made in quantifying the negative pressure which loads the thrombus and in studying the catheters' mechanical behavior, in addition to quantify the mass and number of fragmented clots together with its intrinsic variability. Finally, since the procedures were done with the BCG arresting the flow, no fluid domain was included in the model.

Funding

This project has received funding from the European Union's Horizon 2020 research and innovation program under grant agreement No 777072 and from the MIUR FISR-FISR2019_03221 CECOMES.

CRediT authorship contribution statement

Giulia Luraghi: Writing – original draft, Methodology, Investigation, Conceptualization. **Sara Bridio:** Methodology, Investigation. **Vittorio Lissoni:** Investigation, Formal analysis. **Gabriele Dubini:** Writing – review & editing, Supervision. **Anushree Dwivedi:** Writing – original draft, Methodology. **Ray McCarthy:** Supervision. **Behrooz Fereidoonnezhad:** Writing – original draft, Methodology. **Patrick McGarry:** Supervision. **Frank J.H. Gijsen:** Writing – review & editing, Supervision. **Jose Felix Rodriguez Matas:** Writing – review & editing, Supervision, Conceptualization. **Francesco Migliavacca:** Writing – review & editing, Supervision, Conceptualization.

Declaration of competing interest

The authors declare the following financial interests/personal

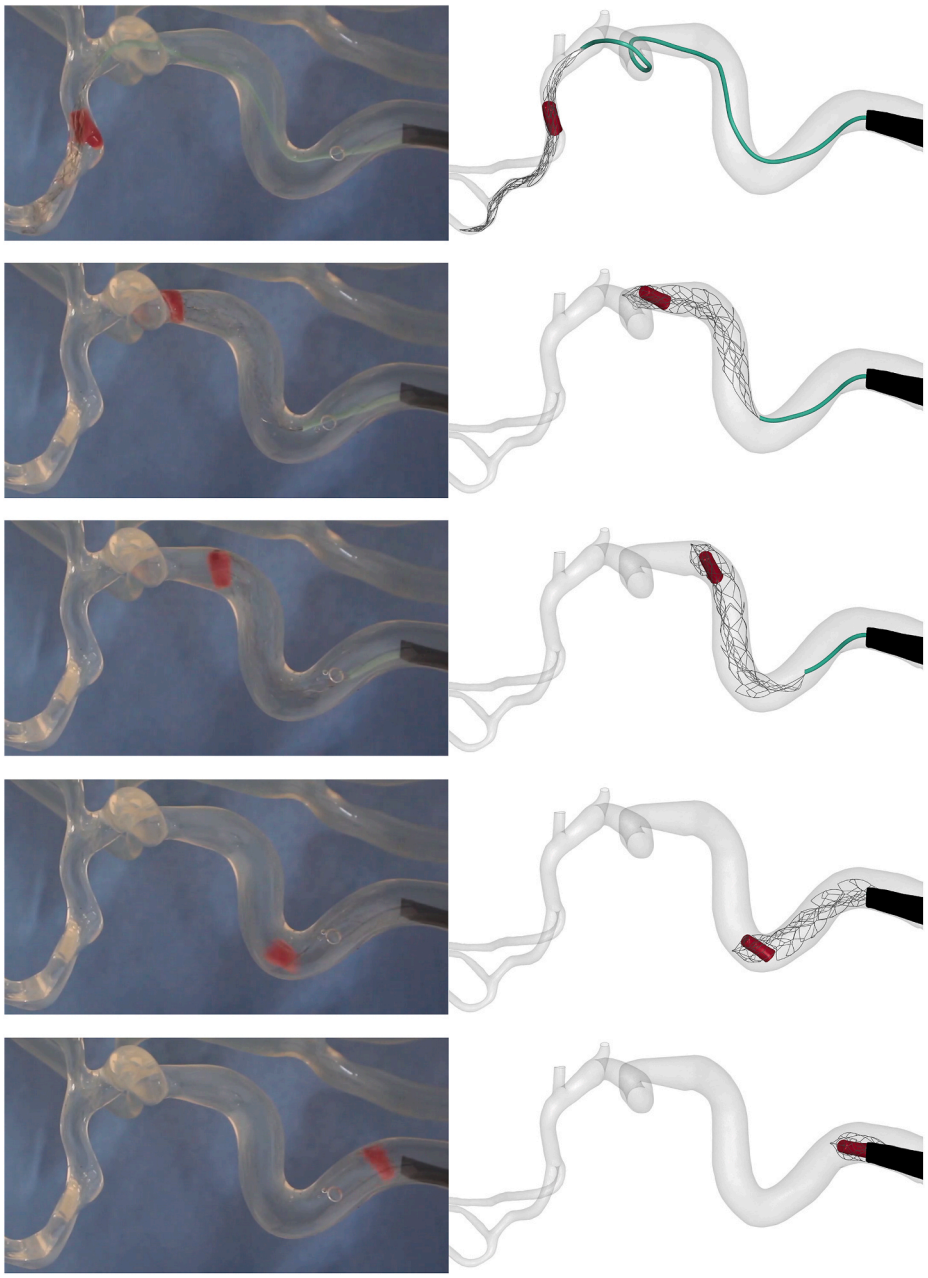

Fig. 5. Comparison between in vitro (left panel) and the in silico (right panel) MT2 test.

relationships which may be considered as potential competing interests: The authors declared the following potential conflicts of interest with respect to the research, authorship, and/or publication of this article: AD and RMC report a financial relationship with Cerenovus outside the submitted work.

Data availability

Data will be made available on request.

Appendix

1 BGC pressure

Computational Fluid Dynamic (CFD) analysis was used to evaluate the fluid dynamic conditions during the aspiration procedure in a simplified internal carotid artery (ICA) shown in Fig. 1A.

The ICA diameter (D_{vessel}) has been varied between 5 and 7 mm, while the clot length (L_{clot}) between 5 and 25 mm The diameter of the clot (D_{clot}) is about 50% to 95% of the vessel diameter (D_{vessel}). The clot and vessel diameter ratio is named as occlusion ratio (X). The catheter here considered is the Neuron Max 088 by Penumbra Inc. with an outer diameter of 8F and inner diameter of 0.088''. The distance between the proximal face of the clot and the catheter tip (d) varies between 0.1 and 10 mm. The physiological ICA pressure of 70 mmHg was applied at the vessel boundaries. The aspiration

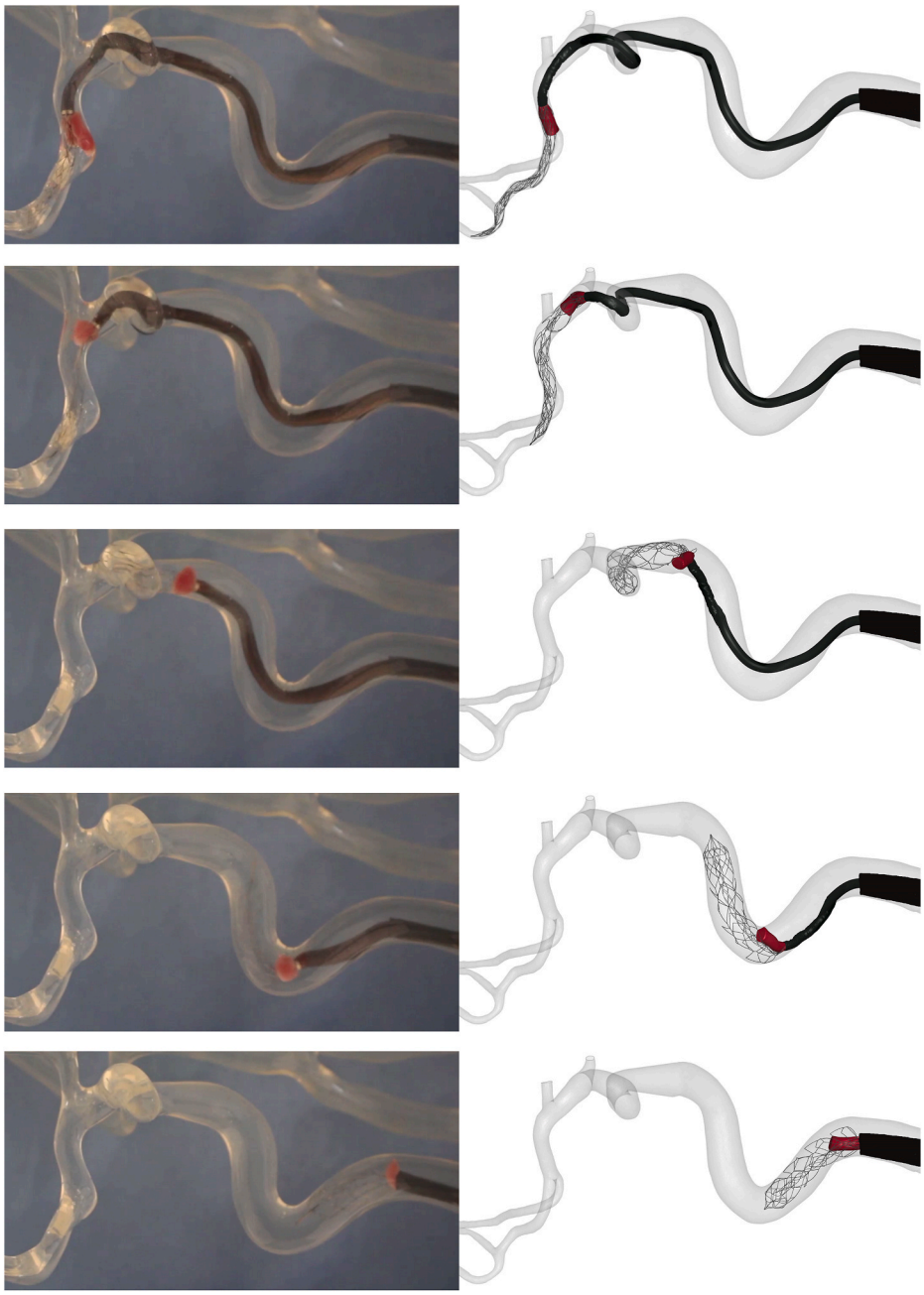

Fig. 6. Comparison between in vitro (left panel) and the in silico (right panel) MT3 test.

pressure varied from 10 to 100 kPa(Chitsaz et al., 2018; Shi et al., 2017). Blood was considered a Newtonian incompressible fluid with a density of 1060 kg/m^3 and viscosity of 3 cP; a k-omega turbulence model was used.

The pressure difference (Δp) between the proximal and distal faces of the clot as a function of the distance between the proximal face of the clot and the aspiration catheter tip was evaluated for each applied aspiration pressure (10, 30, 50, 70, and 100 kPa). The curve with geometrical parameters fitting the model of this paper is shown in Fig. 1Ab (D_{vessel} of 6.5 mm, L_{clot} of 7.5 mm, and X of 0.6).

As shown in Fig. 1Ab, the aspiration pressure acts on the proximal face of the clot only when the distance is short (approximal shorten than 1 mm).

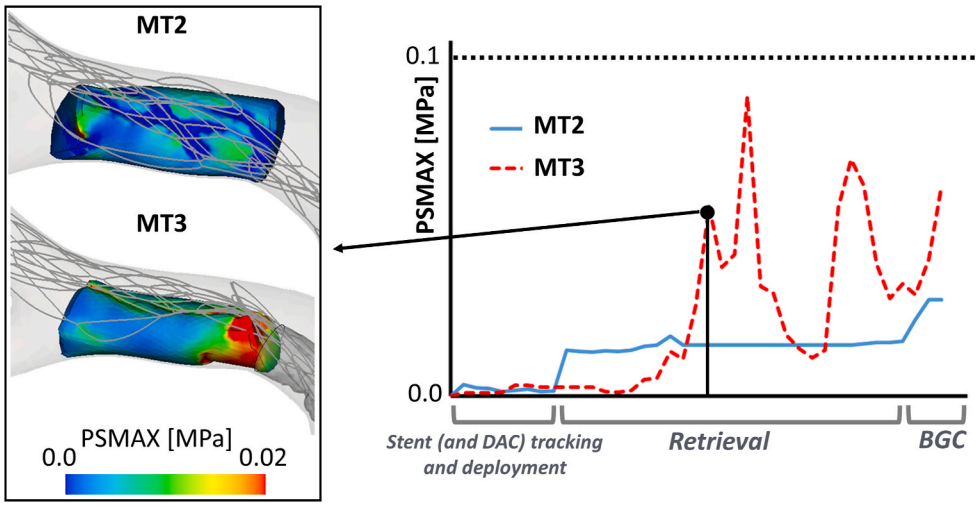

Fig. 7. PSMAX over time during the MT2 and MT3 simulations. A comparison of the PSMAX fields on the thrombus is shown in an instant during the retrieval phase. Discontinuous black line: PSMAX threshold for fibrin-rich thrombi. Fragmentation does not occur during the simulation for both models.

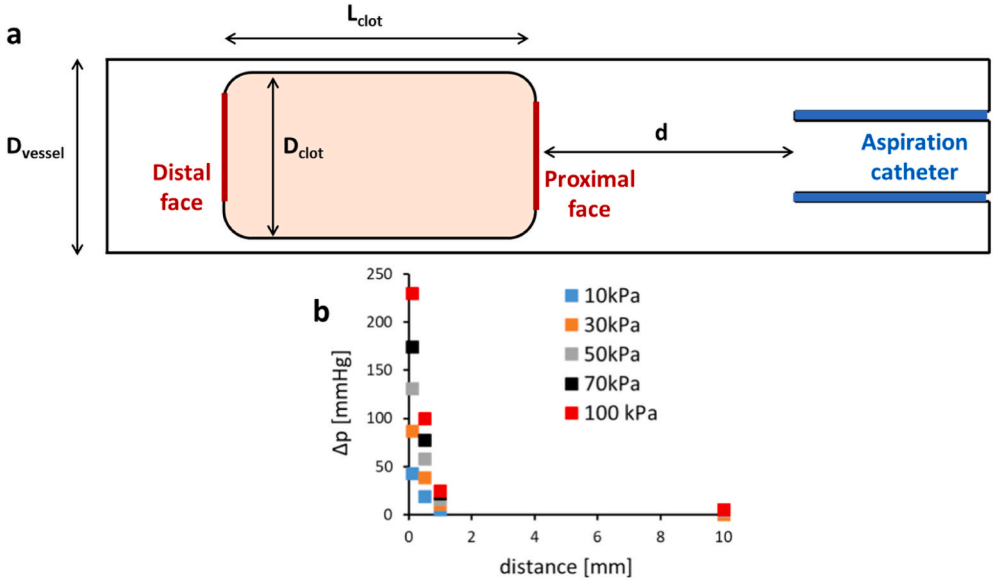

Fig. 1A. geometry of the CFD model (a); pressure difference between the proximal and distal faces of the clot as a function of the distance between the proximal face of the clot and the aspiration catheter tip (b).

2 Material parameters

Table 1A
nitinol material parameters

Parameter	Value
Mass density	6.45 g/cm^3
Austenite elastic modulus	45 GPa
Martensite elastic modulus	17.3 GPa
Poisson's ratio	0.3
Starting stress forward phase transformation	365 MPa
Final stress forward phase transformation	386 MPa
Starting stress reverse phase transformation	197 MPa
Final stress reverse phase transformation	156 MPa
Recoverable strain	0.048

Table 2A
DAC material parameters

Parameter	Value
Mass density	6.45 g/cm^3
Circumferential elastic modulus	3600 MPa
Longitudinal elastic modulus	360 MPa
Poisson's ratio	0.4

References

Berkhemer, O.A., Fransen, P.S.S., Beumer, D., Van den Berg, L.A., Lingsma, H.F., Yoo, A. J., Schonewille, W.J., Vos, J.A., Nederkoorn, P.J., Wermer, M.J.H., van Walderveen, M.A.A., Staals, J., Hofmeijer, J., van Oostayen, J.A., Lycklama à Nijeholt, G.J., Boiten, J., Brouwer, P.A., Emmer, B.J., de Bruijn, S.F., van Dijk, L.C., Kappelle, L.J., Lo, R.H., Van Dijk, E.J., De Vries, J., De Kort, P.L.M., van Rooij, W.J. J., van den Berg, J.S.P., van Hasselt, B.A.A.M., Aerden, L.A.M., Dallinga, R.J., Visser, M.C., Bot, J.C.J., Vroomen, P.C., Eshghi, O., Schreuder, T.H.C.M.L., Heijboer, R.J.J., Keizer, K., Tielbeek, A.V., den Hertog, H.M., Gerrits, D.G., van den Berg-Vos, R.M., Karas, G.B., Steyerberg, E.W., Flach, H.Z., Marquering, H.A., Sprengers, M.E.S., Jenniskens, S.F.M., Beenen, L.F.M., van den Berg, R., Koudstaal, P.J., van Zwam, W.H., Roos, Y.B.W.E.M., van der Lugt, A., van Oostenbrugge, R.J., Majoie, C.B.L.M., Dippel, D.W.J., Investigators, M.C., 2015. A randomized trial of intraarterial treatment for acute ischemic stroke. N. Engl. J. Med. 372, 11–20. https://doi.org/10.1056/NEJMoa1411587.

Bridio, S., Luraghi, G., Rodriguez Matas, J.F., Dubini, G., Giassi, G.G., Maggio, G., Kawamoto, J.N., Moerman, K.M., McGarry, P., Konduri, P.R., Arrarte Terreros, N., Marquering, H.A., van Bavel, E., Majoie, C.B.L.M., Migliavacca, F., 2021. Impact of the internal carotid artery morphology on in silico stent-retriever thrombectomy outcome. Front. Med. Technol. 40. https://doi.org/10.3389/FMEDT.2021.719909.

Chalumeau, V., Blanc, R., Redjem, H., Ciccio, G., Smajda, S., Desilles, J.P., Botta, D., Escalard, S., Boisseau, W., Maïër, B., Labreuche, J., Obadia, M., Piotin, M., Mazighi, M., 2018. Anterior cerebral artery embolism during thrombectomy increases disability and mortality. J. Neurointerventional Surg. 10, 1057–1062. https://doi.org/10.1136/neurintsurg-2018-013793.

Chitsaz, A., Nejat, A., Nouri, R., 2018. Three-dimensional numerical simulations of aspiration process: evaluation of two Penumbra aspiration catheters performance. Artif. Organs 42, E406–E419. https://doi.org/10.1111/aor.13300.

Chueh, J.Y., Kang, D.H., Kim, B.M., Gounis, M.J., 2020. Role of balloon guide catheter in modern endovascular thrombectomy. J. Korean Neurosurg. Soc. 63, 14–25. https://doi.org/10.3340/jkns.2019.0114.

Deshaies, E.M., 2013. Tri-axial system using the Solitaire-FR and Penumbra Aspiration Microcatheter for acute mechanical thrombectomy. J. Clin. Neurosci. 20, 1303–1305. https://doi.org/10.1016/J.JOCN.2012.10.037.

Duffy, S., Farrell, M., McArdle, K., Thornton, J., Vale, D., Rainsford, E., Morris, L., Liebeskind, D.S., MacCarthy, E., Gilvarry, M., 2017. Novel methodology to replicate clot analogs with diverse composition in acute ischemic stroke. J. Neurointerventional Surg. 9, 486–491. https://doi.org/10.1136/neurintsurg-2016-012308.

Dumont, T.M., Mokin, M., Sorkin, G.C., Levy, E.I., Siddiqui, A.H., 2014. Aspiration thrombectomy in concert with stent thrombectomy. J. Neurointerventional Surg. 6 https://doi.org/10.1136/NEURINTSURG-2012-010624.

Fereidoonnezhad, B., Dwivedi, A., Johnson, S., McCarthy, R., McGarry, P., 2021a. Blood clot fracture properties are dependent on red blood cell and fibrin content. Acta Biomater. 127 https://doi.org/10.1016/j.actbio.2021.03.052.

Fereidoonnezhad, B., McGarry, P., 2021. A new constitutive model for permanent deformation of blood clots with application to simulation of aspiration thrombectomy. J. Biomech. 130 https://doi.org/10.1016/J.JBIOMECH.2021.110865, 110865.

Fereidoonnezhad, B., Moerman, K.M., Johnson, S., McCarthy, R., McGarry, P.J., 2021b. A new compressible hyperelastic model for the multi-axial deformation of blood clot occlusions in vessels. Biomech. Model. Mechanobiol. https://doi.org/10.1007/s10237-021-01446-4.

Froehler, M.T., 2017. Comparison of vacuum pressures and forces generated by different catheters and pumps for aspiration thrombectomy in acute ischemic stroke. Interv. Neurol. 6, 199–206. https://doi.org/10.1159/000475478.

Gersh, K.C., Nagaswami, C., Weisel, J.W., 2009. Fibrin network structure and clot mechanical properties are altered by incorporation of erythrocytes. Thromb. Haemostasis 102, 1169–1175. https://doi.org/10.1160/TH09-03-0199.

Good, B.C., Simon, S., Manning, K., Costanzo, F., 2020. Development of a computational model for acute ischemic stroke recanalization through cyclic aspiration. Biomech. Model. Mechanobiol. 19, 761–778. https://doi.org/10.1007/s10237-019-01247-w.

Goyal, M., Demchuk, A.M., Menon, B.K., Eesa, M., Rempel, J.L., Thornton, J., Roy, D., Jovin, T.G., Willinsky, R.A., Sapkota, B.L., Dowlatshahi, D., Frei, D.F., Kamal, N.R., Montanera, W.J., Poppe, A.Y., Ryckborst, K.J., Silver, F.L., Shuaib, A., Tampieri, D., Williams, D., Bang, O.Y., Baxter, B.W., Burns, P.A., Choe, H., Heo, J.-H., Holmstedt, C.A., Jankowitz, B., Kelly, M., Linares, G., Mandzia, J.L., Shankar, J., Sohn, S.-I., Swartz, R.H., Barber, P.A., Coutts, S.B., Smith, E.E., Morrish, W.F., Weill, A., Subramaniam, S., Mitha, A.P., Wong, J.H., Lowerison, M.W., Sajobi, T.T., Hill, M.D., 2015. Randomized assessment of rapid endovascular treatment of ischemic stroke. N. Engl. J. Med. 372, 1019–1030. https://doi.org/10.1056/nejmoa1414905.

Gu, X., Qi, Y., Erdman, A., Li, Z., 2017. The role of simulation in the design of a semi-enclosed tubular embolus retrieval. J. Med. Devices, Trans. ASME 11, 210011–210017. https://doi.org/10.1115/1.4036286.

Gunning, G.M., McArdle, K., Mirza, M., Duffy, S., Gilvarry, M., Brouwer, P.A., 2018. Clot friction variation with fibrin content; implications for resistance to thrombectomy. J. Neurointerventional Surg. 10, 34–38. https://doi.org/10.1136/neurintsurg-2016-012721.

Humphries, W., Hoit, D., Doss, V.T., Elijovich, L., Frei, D., Loy, D., Dooley, G., Turk, A.S., Chaudry, I., Turner, R., Mocco, J., Morone, P., Fiorella, D., Siddiqui, A., Mokin, M., Arthur, A.S., 2015. Distal aspiration with retrievable stent assisted thrombectomy for the treatment of acute ischemic stroke. J. Neurointerventional Surg. 7, 90–94. https://doi.org/10.1136/NEURINTSURG-2013-010986.

Jovin, T.G., Chamorro, A., Cobo, E., de Miquel, M.A., Molina, C.A., Rovira, A., San Román, L., Serena, J., Abilleira, S., Ribó, M., Millán, M., Urra, X., Cardona, P., López-Cancio, E., Tomasello, A., Castaño, C., Blasco, J., Aja, L., Dorado, L., Quesada, H., Rubiera, M., Hernandez-Pérez, M., Goyal, M., Demchuk, A.M., von Kummer, R., Gallofré, M., Dávalos, A., 2015. Thrombectomy within 8 hours after symptom onset in ischemic stroke. N. Engl. J. Med. 372, 2296–2306. https://doi.org/10.1056/NEJMoa1503780.

Kaesmacher, X.J., Boeckh-Behrens, T., Simon, S., Maegerlein, C., Kleine, J.F., Zimmer, C., Schirmer, L., Poppert, H., Huber, T., 2017. Risk of thrombus fragmentation during endovascular stroke treatment. Am. J. Neuroradiol. 38, 991–998. https://doi.org/10.3174/ajnr.A5105.

Kang, D.H., Kim, Y.W., Hwang, Y.H., Park, J., Hwang, J.H., Kim, Y.S., 2013. Switching strategy for mechanical thrombectomy of acute large vessel occlusion in the anterior circulation. Stroke 44, 3577–3579. https://doi.org/10.1161/STROKEAHA.113.002673.

Kolling, S., Du Bois, P.A., Benson, D.J., Feng, W.W., 2007. A tabulated formulation of hyperelasticity with rate effects and damage. Comput. Mech. 40, 885–899. https://doi.org/10.1007/s00466-006-0150-x.

Kühn, A.L., Vardar, Z., Kraitem, A., King, R.M., Anagnostakou, V., Puri, A.S., Gounis, M. J., 2020. Biomechanics and hemodynamics of stent-retrievers. J. Cerebr. Blood Flow Metabol. 40, 2350–2365. https://doi.org/10.1177/0271678X20916002.

Liu, R., Jin, C., Wang, L., Yang, Y., Fan, Y., Wang, W., 2021. Simulation of stent retriever thrombectomy in acute ischemic stroke by finite element analysis. Comput. Methods Biomech. Biomed. Eng. https://doi.org/10.1080/10255842.2021.1976761.

Luraghi, G., Bridio, S., Migliavacca, F., Rodriguez Matas, J.F., 2022. Self-expandable stent for thrombus removal modeling: solid or beam finite elements? Med. Eng. Phys. 106 https://doi.org/10.1016/J.MEDENGPHY.2022.103836.

Luraghi, G., Bridio, S., Miller, C., Hoekstra, A., Felix Rodriguez Matas, J., Migliavacca, F., 2021a. Applicability analysis to evaluate credibility of an in Silico Thrombectomy procedure. J. Biomech. 110631 https://doi.org/10.1016/J.JBIOMECH.2021.110631.

Luraghi, G., Bridio, S., Rodriguez Matas, J.F., Dubini, G., Boodt, N., Gijsen, F.J.H., van der Lugt, A., Fereidoonnezhad, B., Moerman, K.M., McGarry, P., Konduri, P.R., Arrarte Terreros, N., Marquering, H.A., Majoie, C.B.L.M., Migliavacca, F., Felix Rodriguez Matas, J., Dubini, G., Boodt, N., Gijsen, F.J.H., van der Lugt, A., Fereidoonnezhad, B., Moerman, K.M., McGarry, P., Konduri, P.R., Arrarte Terreros, N., Marquering, H.A., Majoie, C.B.L.M., Migliavacca, F., 2021b. The first virtual patient-specific thrombectomy procedure. J. Biomech. 126 https://doi.org/10.1016/J.JBIOMECH.2021.110622, 110622.

Luraghi, G., Cahalane, R.M.E., van de Ven, E., Overschie, S.C.M., Gijsen, F.J.H., Akyildiz, A.C., 2021c. In vitro and in silico modeling of endovascular stroke treatments for acute ischemic stroke. J. Biomech. 127 https://doi.org/10.1016/j.jbiomech.2021.110693, 110693.

Luraghi, G., Rodriguez Matas, J.F., Dubini, G., Berti, F., Bridio, S., Duffy, S., Dwivedi, A., McCarthy, R., Fereidoonnezhad, B., McGarry, P., Majoie, C.B.L.M., Migliavacca, F., 2021d. Applicability assessment of a stent-retriever thrombectomy finite-element model. Interface Focus 11. https://doi.org/10.1098/rsfs.2019.0123, 20190123.

Massari, F., Henninger, N., Lozano, J.D., Patel, A., Kuhn, A.L., Howk, M., Perras, M., Brooks, C., Gounis, M.J., Kan, P., Wakhloo, A.K., Puri, A.S., 2016. ARTS (Aspiration-Retriever technique for stroke): initial clinical experience. Intervent Neuroradiol. 22, 325–332. https://doi.org/10.1177/1591019916632369.

Maus, V., Behme, D., Kabbasch, C., Borggrefe, J., Tsogkas, I., Nikoubashman, O., Wiesmann, M., Knauth, M., Mpotsaris, A., Psychogios, M.N., 2018. Maximizing first-pass complete reperfusion with SAVE. Clin. Neuroradiol. 28, 327–338. https://doi.org/10.1007/s00062-017-0566-z.

McTaggart, R.A., Tung, E.L., Yaghi, S., Cutting, S.M., Hemendinger, M., Gale, H.I., Baird, G.L., Haas, R.A., Jayaraman, M.V., 2017. Continuous aspiration prior to intracranial vascular embolectomy (CAPTIVE): a technique which improves

outcomes. J. Neurointerventional Surg. 9, 1154–1159. https://doi.org/10.1136/NEURINTSURG-2016-012838.

Mousavi, J.S.S.M., Faghihi, D., Sommer, K., Bhurwani, M.M.S., Patel, T.R., Santo, B., Waqas, M., Ionita, C., Levy, E.I., Siddiqui, A.H., Tutino, V.M., 2021. Realistic computer modelling of stent retriever thrombectomy: a hybrid finite-element analysis-smoothed particle hydrodynamics model. J. R. Soc. Interface 18. https://doi.org/10.1098/RSIF.2021.0583, 20210583.

Munich, S.A., Vakharia, K., Levy, E.I., 2019. Overview of mechanical thrombectomy techniques. Clin. Neurosurg. 85, S60–S67. https://doi.org/10.1093/neuros/nyz071.

Neidlin, M., Büsen, M., Brockmann, C., Wiesmann, M., Sonntag, S.J., Steinseifer, U., Kaufmann, T.A.S., 2016. A numerical framework to investigate hemodynamics during endovascular mechanical recanalization in acute stroke. Int. j. numer. method. biomed. eng. 32 https://doi.org/10.1002/cnm.2748 e02748.

Nikoubashman, O., Wischer, D., Hennemann, H.M., Büsen, M., Brockmann, C., Wiesmann, M., 2018. Under pressure: comparison of aspiration techniques for endovascular mechanical thrombectomy. Am. J. Neuroradiol. 39, 905–909. https://doi.org/10.3174/ajnr.A5605.

Ospel, J.M., Volny, O., Jayaraman, M., McTaggart, R., Goyal, M., 2019. Optimizing fast first pass complete reperfusion in acute ischemic stroke–the BADDASS approach (BAlloon guiDe with large bore Distal Access catheter with dual aspiration with Stent-retriever as Standard approach). Expet Rev. Med. Dev. 16, 955–963. https://doi.org/10.1080/17434440.2019.1684263.

Oyekole, O., Simon, S., Manning, K.B., Costanzo, F., 2021. Modeling acute ischemic stroke recanalization through cyclic aspiration. J. Biomech. 128 https://doi.org/10.1016/j.jbiomech.2021.110721, 110721.

Saver, J.L., Goyal, M., Bonafe, A., Diener, H.-C., Levy, E.I., Pereira, V.M., Albers, G.W., Cognard, C., Cohen, D.J., Hacke, W., Jansen, O., Jovin, T.G., Mattle, H.P., Nogueira, R.G., Siddiqui, A.H., Yavagal, D.R., Baxter, B.W., Devlin, T.G., Lopes, D.K., Reddy, V.K., du Mesnil de Rochemont, R., Singer, O.C., Jahan, R., 2015. Stent-retriever thrombectomy after intravenous t-PA vs. t-PA alone in stroke. N. Engl. J. Med. 372, 2285–2295. https://doi.org/10.1056/NEJMoa1415061.

Shi, Y., Cheshire, D., Lally, F., Roffe, C., 2017. Suction force-suction distance relation during aspiration thrombectomy for ischemic stroke: a computational fluid dynamics study. Phys. Med. 3, 1–8. https://doi.org/10.1016/j.phmed.2016.11.001.

Talayero, C., Romero, G., Pearce, G., Wong, J., 2020. Thrombectomy aspiration device geometry optimization for removal of blood clots in cerebral vessels. J. Mech. Eng. Sci. 14, 6229–6237. https://doi.org/10.15282/jmes.14.1.2020.02.0487.

Wang, W., Wan, Z., Wu, B., Lu, L., Tang, Y., 2019. Finite element analysis for mechanics of guiding catheters in transfemoral intervention. J. Card. Surg. 34, 690–699. https://doi.org/10.1111/JOCS.14132.

Weafer, F.M., Duffy, S., Machado, I., Gunning, G., Mordasini, P., Roche, E., McHugh, P. E., Gilvarry, M., 2019. Characterization of strut indentation during mechanical thrombectomy in acute ischemic stroke clot analogs. J. Neurointerventional Surg. 11, 891–897. https://doi.org/10.1136/neurintsurg-2018-014601.